Volumes 211–212 • 15 November 2012 • Issn 1385-8947

ELSEVIER

CHEMICAL ENGINEERING JOURNAL

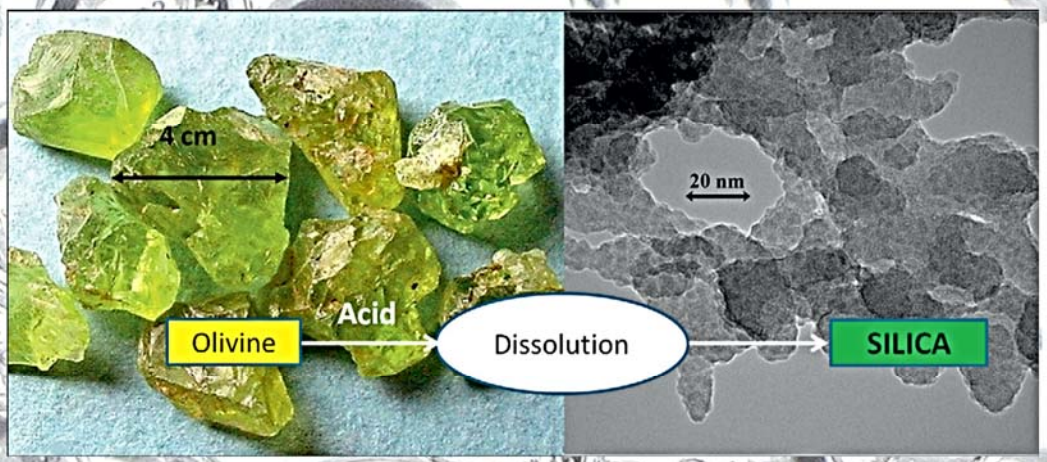

FEATURED ARTICLE

MATERIALS SYNTHESIS PROCESSING

The properties of amorphous nano-silica synthesized by the dissolution of olivine

A. Lazaro, H.J.H. Brouwers, G. Quercia, J.W. Geus

Design prepared by A. Lazaro and A. Taher.

Chemical Engineering Journal 211-212 (2012) 112–121

Contents lists available at SciVerse ScienceDirect

Chemical Engineering Journal

journal homepage: www.elsevier.com/locate/cej

The properties of amorphous nano-silica synthesized by the dissolution of olivine

A. Lazaro [a,*], H.J.H. Brouwers [a], G. Quercia [a,b], J.W. Geus [c]

[a] Department of the Built Environment, Eindhoven University of Technology, P.O. Box 513, 5600 MB Eindhoven, The Netherlands
[b] Materials innovation institute (M2i), Delft, The Netherlands
[c] Debye Institute for Nanomaterials Science, University of Utrecht, Utrecht, The Netherlands

HIGHLIGHTS

- The dissolution of olivine produces an amorphous nano-silica of high quality.
- The SSA of this nano-silica is between 100 and 300 m^2/g.
- Olivine nano-silica has primary particles of 10–25 nm agglomerated in clusters.
- Olivine nano-silica is mesoporous with an average pore size around 20 nm.
- The texture of this silica depends on the olivine kinetics and the washing steps.

GRAPHICAL ABSTRACT

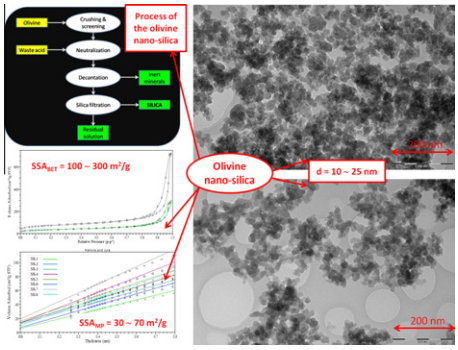

ARTICLE INFO

Article history:
Received 6 June 2012
Received in revised form 23 August 2012
Accepted 14 September 2012
Available online 24 September 2012

Keywords:
Amorphous mesoporous nano-silica
Synthesis
Olivine
Specific surface area

ABSTRACT

This study addresses the synthesis of amorphous mesoporous nano-silica by the dissolution of olivine in sulfuric acid, showing the influence of the process conditions on the properties of nano-silica. The olivine dissolution process is a convenient alternative to the traditional methods of nano-silica production; and that is because the low energy requirement makes it possible to use this material in new fields where previously its price was prohibitive. The produced nano-silica has a specific surface area between 100 and 300 m^2/g and a particle size between 10 and 25 nm. These particles are agglomerated in clusters forming a mesoporous material with an average pore diameter around 20 nm. The impurity content is below 5%, and the silica yield of the process in the range of 54–83%. When the separation of the silica is carried out by filtration, the textural properties of the material have a direct influence on the separation efficiency. The texture and specific surface area of nano-silica depends on several factors of the process, the main ones being the kinetics of the dissolution of olivine and the washing steps of the nano-silica. Thus, the properties of this nano-silica can be tailored by changing the process conditions.

1. Introduction

At present a wide range of silica products are manufactured industrially for various applications. Silicas are mainly used for reinforcement of elastomer products, thickening of liquid systems such as paints, thermosetting resins, and printing inks, and as fillers in silicone rubber [1]. World demand for specialty silicas, which includes precipitated silica, fumed silica, silica gel and silica sol, was 1.9 million metric tons in 2009 and will rise to 2.7 million metric tons in 2014 with a total value of $5.8 billion [2], making it one of the most used nano-materials. Nowadays, the two most important commercial processes in the production of nano-silica are the neutralization of sodium silicate solutions with acid (this material is referred as precipitated silica) and the flame hydrolysis (pyrogenic silica). Both processes are expensive because of the price of the raw materials and the energy requirements. Nano-silica could be applied even more widely if a new industrial, low cost, production process could be developed.

* Corresponding author. Tel.: +31 (0)40 247 3411.
E-mail address: a.lazaro.garcia@tue.nl (A. Lazaro).

1385-8947/$ - see front matter © 2012 Elsevier B.V. All rights reserved.
http://dx.doi.org/10.1016/j.cej.2012.09.042

Nomenclature

Roman

d	diameter (μm) or (nm)
E	efficiency (%)
$[H^+]$	concentration of hydrogen ions (mol/l)
LOI	loss of ignition (% in mass)
m	mass (g)
M	molar mass (g/mol)
n	number of moles (moles)
P	purity (%)
RSD	relative standard deviation (%)
SSA	specific surface area (m^2/g)
t	time (h)
T	temperature (°C)
X	conversion (%)
Y	yield (%)

Greek

ρ	density (g/cm^3)

Subscripts

BET	Brunaer, Emmett and Teller
E	external
exp	experimental
i	initial
im	impurity
$[H^+]$	hydrogen ions
MP	micropore
neu	neutralized
NS	nano-silica
ol	olivine
ol_unr	olivine unreacted
p	pore size
p_A	pore size calculated during the adsorption branch
p_D	pore size calculated during the desorption branch
r	reaction
Si	silica
sep	separation
t	time
T	total
th	theoretical

Initial research [3–10] has demonstrated that nano-silica can be produced by dissolving olivine in acids following Eq. (1). Olivine, $(Mg, Fe)_2SiO_4$, is the fastest weathering silicate and the Si–O–Si bonds are broken more easily than in any other silicate mineral.

$$(Mg, Fe)_2SiO_4 + 4H^+ \rightarrow Si(OH)_4 + 2(Mg, Fe)^{2+}. \quad (1)$$

The neutralization yields a mixture of a magnesium/iron salt solution, precipitated silica, unreacted olivine and inert minerals. Once the reaction is complete, the unreacted materials and inert minerals are removed from the final suspension by sedimentation. Subsequently, the silica can be separated from the resulting mixture by washing and filtering.

The product of the dissolution of olivine is a colloidal solution containing magnesium sulfate, iron (II) sulfate, colloidal silica and nonreactive minerals. The colloidal chemistry of silica strongly depends on the amount of salt and the pH of the solution. At the pH conditions of olivine silica (−0.5 to 1), a colloidal solution is usually unstable and the silica particles agglomerate and flocculate [11,12]. The speed of agglomeration of silica particles is catalyzed by the hydrogen ion [11,12]. The texture of nano-silica is a complex topic reviewed by several researchers [13–16], but only Lieftink [5,16] studied in depth the nano-silica produced from olivine.

Although the research of Lieftink [5] provided interesting results, more data about the following items are desired: (i) the effects of the process variables (surface area of olivine, hydrogen ion activity and temperature) on the textural properties of the resulting nano-silica; (ii) the influence of the mode of operation on the process, particularly on the process yield; (iii) the chemical composition of nano-silica produced in order to establish the impurities left.

The main purpose of this research is to verify the good properties of the nano-silica synthesized (high specific surface area, mesoporosity and low content of impurities), in order to prove that amorphous mesoporous nano-silica can be produced satisfactorily by the dissolution of olivine in acid. An additional aim of this work is to present new data and more details about the influence of the process conditions on the textural properties (size of the primary particles and size and shape of the agglomerates), the separation efficiency, and the content of impurities of the nano-silica produced.

The experiments conducted in our research showed that nano-silica can be produced by the dissolution of olivine. The nano-silica produced is mesoporous, presenting impurities below 5% and a specific surface area between 100 and 300 m^2/g. The cost of this nano-silica should be lower than the nano-silica produced by the commercial methods due to the low price of the raw materials and the low energy requirement of this method (the temperature is around 70 °C and the reaction is exothermic). Therefore, the olivine nano-silica could be applied in new fields where it is now limited due to its price.

2. Texture of the olivine nano-silica

The main author in this area, Lieftink [5], studied the texture of the silica produced by the dissolution of olivine, and he showed that variation of the production rate and the total reaction time led to different silica textures. Thus, the silica texture generated during the reaction of olivine is mostly determined by the dissolution rate of olivine. Olivine dissolution has been widely studied [4,6,17–23], but only Jonckbloedt [6] studied it in the olivine nano-silica conditions. He stated that the dissolution of olivine in these conditions is controlled by surface reactions and that it depends on the surface area of olivine, hydrogen ion activity and temperature [6]. Thus, increasing the surface area of olivine, the hydrogen ion activity and the reaction temperature will increase the reaction rate.

Experiments carried out by Lieftink [5] showed that when the dissolution of olivine exhibited a slow rate, particle growth occurred; and when the dissolution proceeded rapidly, particle growth occurred as well, but slower. Particle growth proceeded according to a particle agglomeration model, which means that the final particle size was determined by the rate of formation of 2 nm particles and the agglomeration of these particles. Therefore, when 2 nm particles were produced rapidly, the probability of agglomeration of two small particles was larger than the probability of accommodation of small particles into a larger, growing particle.

Table 1
Surface area of the olivine nano-silica by Lieftink [5].

T (°C)	Coarse (425–1000 μm)			Fine (90–425 μm)		
	SSA_{BET} (m^2/g)	SSA_E (m^2/g)	t_r (h)	SSA_{BET} (m^2/g)	SSA_E (m^2/g)	t_r (h)
40	140	110	145.8	227	151	71.7
50	–	–	62.5	–	–	7.2
70	280	186	22.5	310	209	5.7
90	340	263	4.3	399	312	2.5

Another factor which influences the texture of nano-silica, especially the specific surface area, is the amount of magnesium sulfate. The separation and washing of the olivine nano-silica increases the specific surface area and the pore volume. Washing does not affect the texture of the silica, but removes the magnesium sulfate from the pores. Therefore, the washing of olivine nano-silica can be considered as the extraction of magnesium sulfate from the porous system. Lieftink [5] reported that seven washing steps of 100 ml of demineralized water were needed to remove almost all magnesium sulfate from 750 ml of colloidal nano-silica, increasing the surface area from 50 to 300 m^2/g.

The specific surface area (SSA_{BET}), the external specific surface area (SSA_E) and the reaction time (t_r) of the olivine nano-silica surface produced by Lieftink [5] at different temperatures are presented in Table 1, where the terms coarse and fine refer to the particle size of olivine. This olivine nano-silica presented a SSA_{BET} in the range of 140–400 m^2/g and exhibited micropores, mesopores and macropores.

3. Process yield of the olivine nano-silica

The process yield, Y_{NS}, is defined as the rate between the nano-silica produced experimentally, $NS_{\_exp}$, and the potential nano-silica present in the olivine calculated theoretically, $NS_{\_th1}$,

$$Y_{NS}\ (\%) = \frac{m_{NS\_exp}}{m_{NS\_th1}} \times 100. \tag{2}$$

The theoretical nano-silica is expressed as

$$m_{NS\_th1} = m_{ol} \times M_{SiO_2} \times M_{ol}, \tag{3}$$

where m_{ol} is the mass of olivine, M_{SiO_2} is the molecular weight of silica and M_{ol} is the molecular weight of olivine. The m_{NS_exp} is calculated with

$$m_{NS\_exp} = m_{NS\_exp\_im} \times m_{SiO_2}, \tag{4}$$

where $m_{NS\_exp\_im}$ is the impure mass of nano-silica dried at 120 °C and m_{SiO_2} is the silica content of the dried material and can be determined if we know the other compounds present in the material. Besides silica, silanol groups, physisorbed water and sulfates can also be found in this dried nano-silica.

When the silica is thermally treated, the physisorbed water is removed at about 150 °C. At 200 °C, all the physisorbed water from the surface is gone, but all the silanol groups still remain. Above this temperature, silanol groups condense, releasing water given by

$$Si{-}OH + Si{-}OH \rightarrow Si{-}O{-}Si + H_2O. \tag{5}$$

This happens in three different steps: (i) at 450–500 °C vicinal groups condense; (ii) at 600–800 °C internal silanol groups condense; and (iii) up to about 1000–1100 °C, only isolated silanol groups remain on the silica surface [24]. Iron and magnesium sulfate decompose around 460 and 800 °C [25], respectively; and sulfuric acid decomposes at 340 °C [26].

The silica content, m_{SiO_2}, can be calculated from the thermogravimetric analysis (TGA) as the difference between the final mass of the TGA at 1100 °C and the oxide content with

$$m_{SiO_2}(\%) = (m_{1100} - m_{MgO} - m_{FeO}) \times (100 - m_{20-120}), \tag{6}$$

where m_{20-120} is the mass loss in the interval 20–120 °C due to the release of water adsorbed on the nano-silica.

Another important parameter of the process is the separation efficiency, E_{Sep}, defined as the rate between the nano-silica produced experimentally and the potential nano-silica produced from the reacted olivine, $NS_{\_th2}$,

$$E_{Sep}\ (\%) = \frac{m_{NS\_exp}}{m_{NS\_th2}} \times 100. \tag{7}$$

In this case the theoretical nano-silica is expressed as

$$m_{NS\_th2}(g) = n_{H\_neu} \times M_{SiO_2} \times 4, \tag{8}$$

where n_{H_neu} is the amount of protons neutralized.

Generally, the process yield depends on the conversion factor of the reaction and on the separation efficiency of post-reaction treatments. Because in the olivine nano-silica process almost all the olivine has reacted with sulfuric acid, the yield depends mainly on the amount of nano-silica lost in the separation steps. When the separation is performed by filtration, which is the most common method to separate the silica from the sulfate salts, the process yield depends on the time required to produce the silica cake and the properties of the silica cake. For the olivine nano-silica process, Jonckbloedt [6] reported a production of 65 g of nano-silica per kg of 3 M sulfuric acid and 190 g of olivine, resulting in a separation efficiency of 67%. This value is calculated from the amount of $[H^+]$ neutralized because no data about the purity of olivine was reported.

4. Experimental method

The ground olivine rock used in this study was Oliflux, which was supplied by North Cape Mineral (Norway). The desired grain size fractions were obtained by wet-sieving. Then, the sieve fractions were ultrasonically treated with ethanol to remove any adhering fines. The main mineral detected by X-ray diffraction (XRD) was olivine. Others silicates, oxides and carbonates were present in small quantities as well. The chemical composition of the olivine was determined by X-ray fluorescence (XRF) analysis, and the mineralogical composition was calculated from the XRD and XRF analysis. Approximately 88.7 mass percentage of the rock was olivine with the composition $(Mg_{1.84}Fe_{0.153}Ni_{0.007})SiO_4$, with a forsterite content of 92% (normally expressed as FO_{92}) and a molar mass of 145.7 g/mol.

Experiments were carried out at the following temperatures: 50, 70 and 90 °C and with a fraction size of 125–150, 250–300 and 500–600 μm in a vigorously stirred double-wall glass reactor of one liter. The temperature was kept constant by circulating water from a thermostat through the double wall. Particularly at the beginning of an experiment, the control of the temperature was rather difficult, resulting in an oscillation of up to 3 °C in the fastest experiments. The reagents used were 500 ml of 3 M sulfuric acid and stoichiometric amount of olivine, previously dried. The concentration of hydrogen ions was determined by titration with a 0.05 M $Na_2B_4O_7$ solution at regular time intervals. The

neutralization reaction continued until the [H+] was below 0.1 mol/l when it was stopped. After that, the stirrer was switched off and the slurry was left for 10 min, after which the solution was separated from the solid residue by sedimentation. Subsequently, the remaining slurry was washed with 500 ml of 0.1 M sulfuric acid solution and filtered over a Buchner funnel. Sulfuric acid was chosen as the rinsing liquid to prevent oxidation of the iron. The washing and filtering processes were repeated four times, except in cases where too much silica escaped with the filtrate.

The nano-silica produced was characterized by inductively coupled plasma mass spectrometry (ICP-MS), combustion infrared analysis, thermogravimetric (TG) analysis, gas physisorption and transmission electron microscopy (TEM).

The chemical analyses were carried out with an ICP-MS X2 Thermo Scientific equipment and a Leco SC 632 (combustion infrared analysis). An STA 449 F1 Jupiter (Netzsch Instruments) was used to perform the TG analysis. The temperature was increased gradually from room temperature to 1100 °C at 1 °C/min, keeping it constant for 2 h at 200 °C and 1100 °C, respectively.

A Micromeritics TriStar 3000 equipment using N_2 and with a soaking time of 240 min at 120 °C was used for the gas physisorption analysis [27]. The specific surface area, SSA_{BET}, the specific micropore surface area, SSA_{MP}, and the pore size distribution were calculated using the BET [28], *t*-plot [29,30] and BHJ methods [31], respectively. The physisorption analyses were carried out three times with a standard deviation below 5% for the SSA_{BET}. The specific external surface area, SSA_E, was determined as the difference between the specific surface area and the specific micropore surface area. The particle size of the nano-silica was calculated from the geometrical relationship between surface area and mass given by

$$d(\text{nm}) = \frac{6000}{\text{SSA} \times \rho}, \tag{9}$$

where d is the particle size of nano-silica considered to be spherical (nm), ρ the density of the material, 2.2 (g/cm^3) for nano-silica, and SSA the surface area (m^2/g). This particle size is an average value, considering that the particles are spherical. Lieftink [5] stated that the correlation between the primary particle size, obtained from the TEM images and the SSA_E, is in good agreement for olivine nano-silica. Depending on the surface area used (SSA_{BET} or SSA_{EXT}) in Eq. (9), different values of particle sizes are obtained (d_{BET} or d_{EXT}). These particle sizes would only be the same if the material analyzed did not feature microporosity.

5. Experimental results

5.1. Experimental conditions

The experiments carried out are shown in Table 2 together with the amount of reagents used ($m_{H_2SO_4}$ and m_{ol}), molecular ratio of hydrogen ions/olivine, average particle size of olivine, d_{ol}, and reaction temperature, T_r. Fig. 1 presents the neutralization curve of the sulfuric acid for experiment NS-8. The neutralization curves of the other experiments show a similar trend, but with different reaction times.

Table 2
Initial conditions of the olivine nano-silica experiments.

Sample	$m_{H_2SO_4}$ (g)	$m_{olivine}$ (g)	Ratio H+/Ol	d_{ol} (μm)	T_r (°C)
NS-1	589.1	109.8	4.5	138	48.7
NS-2	593.5	125.0	4.0	200	52.0
NS-3	555.8	121.7	3.8	400	55.0
NS-4	532.7	112.6	4.0	313	70.2
NS-5	593.9	122.9	4.0	400	70.7
NS-6	594.2	113.1	4.4	550	69.9
NS-7	593.7	119.4	4.2	275	87.7
NS-8	592.3	121.5	4.1	400	86.2

3 M sulfuric acid was used in all the experiments.

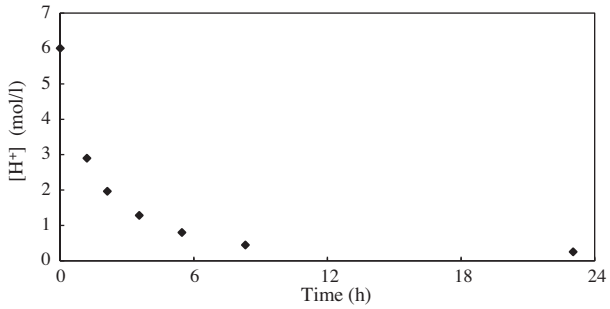

Fig. 1. Neutralization curve of the NS-8 experiment.

Table 3 shows the key parameters for the production of nano-silica. These parameters are the $[H^+]_{final}$ at which the reaction was stopped, the reaction time, t_r, the time required to reach [H+] of 1 mol/l, the aging time, the amount of unreacted olivine, m_{ol_unr}, olivine conversion, X_{ol}, and the filtration steps. The aging time was calculated as the difference between the total reaction time and the time when 90% of the olivine was consumed.

5.2. Kinetics and reaction time

While the purpose of this article is not to study the kinetics of the dissolution of olivine under these acidic conditions, some comments are required, because the kinetics influence the properties of the nano-silica. As was mentioned previously, the kinetics of the dissolution of olivine depends on the specific surface area of olivine, hydrogen ion activity, and temperature. The particle size of olivine was used instead of the surface area because of its simplicity. The times required to reach the [H+] of 1 mol/l versus the particle size of olivine at the different temperatures are plotted in Fig. 2.

The reaction time required decreased when the temperature increased and when the average particle size of olivine declined. This change is in agreement with the kinetics of the dissolution of olivine. The value of the reaction time required for the NS-1 experiment was not represented in this figure. This reaction time was unexpectedly long compared with the rest of the experiments at 50 °C, because the ratio (H+/Ol) was too high and also because the temperature was the lowest. The high ratio of (H+/Ol) was due to smaller amount of olivine used in this experiment, which means that most of the olivine is consumed and the pH is still significantly high.

For industrial applications, the synthesis process can be carried out under fast kinetic conditions to decrease the required reaction time. Only 3 h are required to produce nano-silica at 87 °C, which is a reasonable reaction time. The reaction time can be reduced even further by operating at higher temperatures and higher H+/Ol ratios.

5.3. Properties of the olivine nano-silica

The adsorption isotherms and the *t*-plot curves of the experiments NS-1 and NS-7 are plotted in Figs. 3 and 4, respectively. The adsorption isotherm NS-1 and NS-7 were selected as the samples with the lowest and the highest SSA_{BET}, respectively. The adsorption isotherm curves of all the olivine nano-silicas are similar in shape, but the volumes of gas adsorbed are higher for samples of higher specific surface areas.

The adsorption isotherm of olivine nano-silica can be classified as type IV with H1 hysteresis loop [32,33]. This adsorption

Table 3
Parameters of the production of olivine nano-silica.

Sample	$[H^+]_{final}$ (mol/l)	t_r (h)	t_r $[H^+]$ = 1 M (h)	$Aging_t$ (h)	M_{ol_unr} (g)	X_{ol} (%)	Filt. steps
NS-1	0.93	46.0	43.4	11.5	4.6	95.1	2
NS-2	0.24	71.0	29.7	35.8	5.0	95.4	4
NS-3	0.31	75.0	37.2	5.9	10.0	90.6	3
NS-4	0.23	19.2	5.8	10.6	4.5	95.4	4
NS-5	0.27	42.2	10.1	25.3	3.7	96.6	4
NS-6	0.65	63.7	33.6	32.6	1.4	98.3	4
NS-7	0.62	6.0	3.5	1.9	4.9	93.5	4
NS-8	0.25	23.0	4.7	17.2	2.3	97.8	3

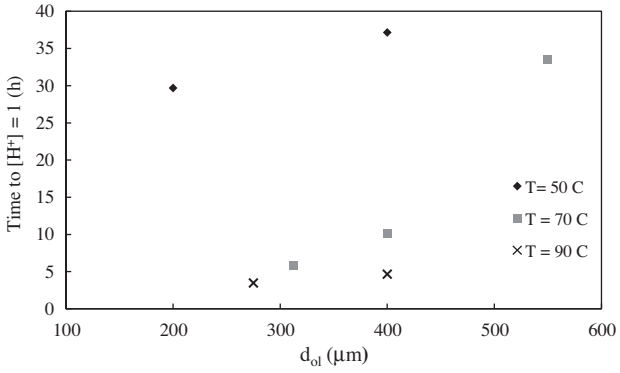

Fig. 2. Time to reach $[H^+]$ of 1 M versus the average particle size of olivine.

isotherm is typical for mesoporous materials and is related to capillary condensation taking place in mesopores [32]. Hysteresis H1 is associated with porous materials consisting of agglomerates with narrow pore distributions [32].

Table 4 shows the values of the surface area, the average pore size, the average particle size and the ratio between SSA_{MP} and SSA_{BET} of the olivine nano-silica. The specific surface areas for samples produced at 70 and 90 °C, and samples produced at 50 °C are shown in Figs. 5 and 6, respectively. As Lieftink stated [5], the SSA of the olivine nano-silica increases with the faster reaction of olivine. That means, the SSA of nano-silica rises with the reaction temperature, the SSA of olivine and the $[H^+]$. This trend can be observed in Fig. 5. However, Fig. 6 does not exhibit this trend. The reasons are that the temperature in these experiments (experiments NS-1, NS-2, and NS-3) was not constant (being in the range

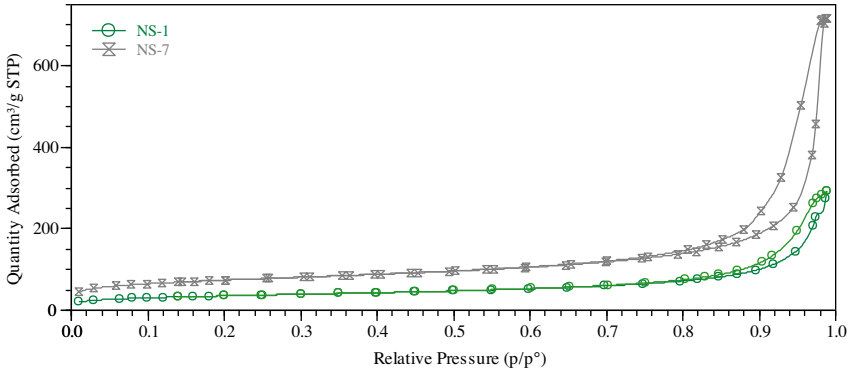

Fig. 3. Adsorption isotherms of the olivine nano-silica NS-1 and NS-7.

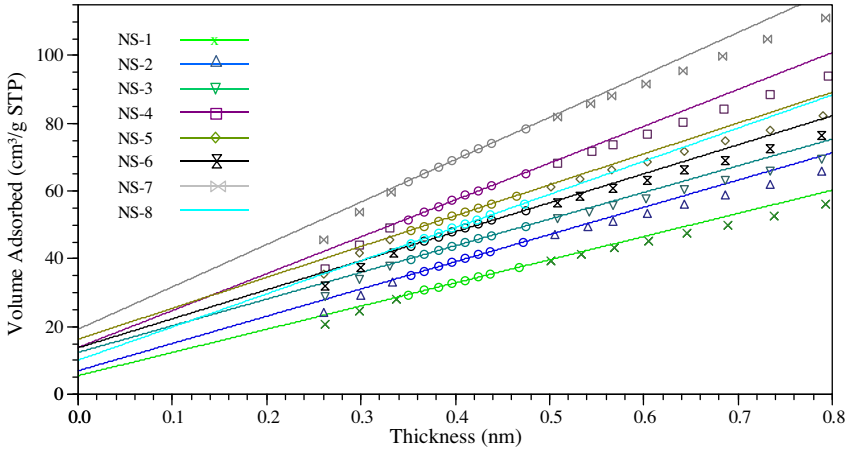

Fig. 4. *t*-plot curves of olivine nano-silica.

Table 4
Surface area, pore size, particle size and ratio SSA_{MP}/SSA_{BET} of the olivine nano-silica.

Sample	SSA_{BET} (m^2/g)	SSA_{MP} (m^2/g)	SSA_E (m^2/g)	d_{p_A} (nm)	d_{p_D} (nm)	d_{BET} (nm)	d_E (nm)	SSA_{MP}/SSA_{BET} (%)
NS-1	131	27	104	21	21	26	21	21
NS-2	150	27	123	18	17	22	18	18
NS-3	165	43	122	18	18	22	17	26
NS-4	218	52	166	18	17	16	13	24
NS-5	198	58	139	19	19	20	14	29
NS-6	179	47	132	28	24	21	15	27
NS-7	266	72	194	25	22	14	10	27
NS-8	185	36	149	18	17	18	15	19

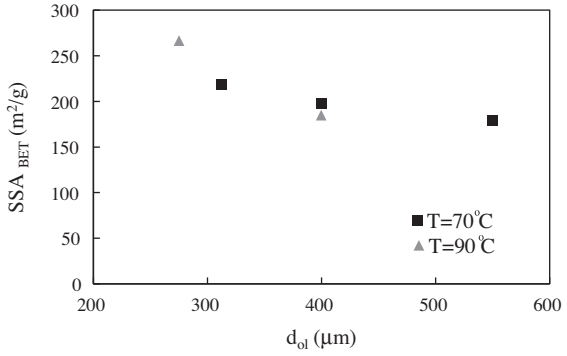

Fig. 5. Specific surface area of olivine nano-silica against the particle size of olivine for experiments at 70 and 90 °C.

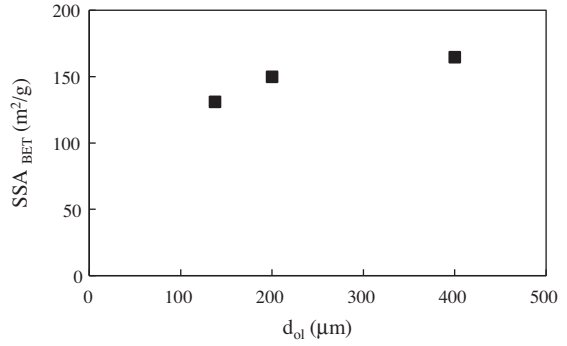

Fig. 6. Specific surface area of olivine nano-silica against the particle size of olivine for experiments at 50 °C.

of 48–55 °C), the final concentration of $[H^+]$ was slightly different, but most importantly, the number of filtration steps was not constant. In the experiment NS-1, so much silica was being removed during the washing steps that we decided to stop the cleaning after the second step. A considerable amount of magnesium sulfate was, therefore, still in the nano-silica pores (as can been seen in Table 5), presenting an SSA_{BET} lower than expected for clean nano-silica.

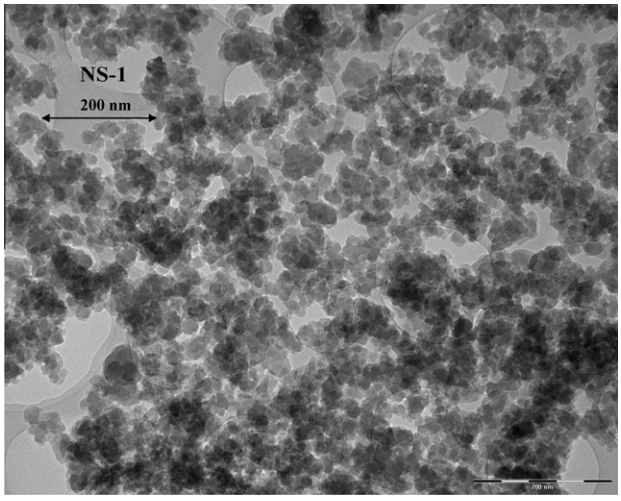

Fig. 7. TEM picture (89 kx) of the olivine nano-silica NS-1.

Sample NS-3 resulted in a larger surface area, because the temperature was 55 °C and because the ratio H^+/Ol was slightly lower than in the other two experiments. Because all the experiments were done at the same initial concentration of sulfuric acid, the lower ratio of H^+/Ol indicates that the surface area of olivine was higher, increasing the kinetics and the specific surface area of the silica as well.

TEM images (89 kx magnification) are shown in Figs. 7 and 8, for NS-1 and NS-7, respectively. Figs. 7 and 8 show a material of particle size between 10 and 50 nm, with angular shape. The highly agglomerated state, typical for silicas produced at low pH, can be seen in both silicas. This highly agglomerated state is because below the isoelectric point silica particles agglomerate, and the agglomeration is catalyzed by the hydrogen ion [11,12]. Sample NS-1 was more agglomerated than sample NS-7 probably because in experiment NS-1 the reaction times was longer, giving more time to the silica to agglomerate.

The primary particle size of the silicas (Eq. (9)) derived from the SSA is in the range of 14–26 and of 10–21 nm for d_{BET} and d_E,

Table 5
Chemical analysis (in mass%) of the olivine nano-silica.

Sample	S (%)	Na (%)	Mg (%)	Al (%)	Ca (%)	Cr (%)	Fe (%)	Ni (%)	P_{Si} (%)
NS-1	3.89	0.00	1.88	0.02	0.05	0.00	0.36	0.02	86.01
NS-2	1.18	0.00	0.18	0.01	0.03	0.00	0.04	0.00	96.20
NS-3	1.26	0.01	0.29	0.02	0.08	0.00	0.06	0.00	95.76
NS-4	1.17	0.00	0.16	0.01	0.03	0.00	0.03	0.00	96.26
NS-5	1.19	0.00	0.26	0.02	0.04	0.00	0.05	0.00	96.06
NS-6	0.92	0.02	0.39	0.04	0.05	0.01	0.05	0.00	96.68
NS-7	1.36	0.00	0.28	0.02	0.04	0.00	0.06	0.00	95.52
NS-8	2.16	0.00	0.96	0.03	0.03	0.00	0.15	0.01	92.34

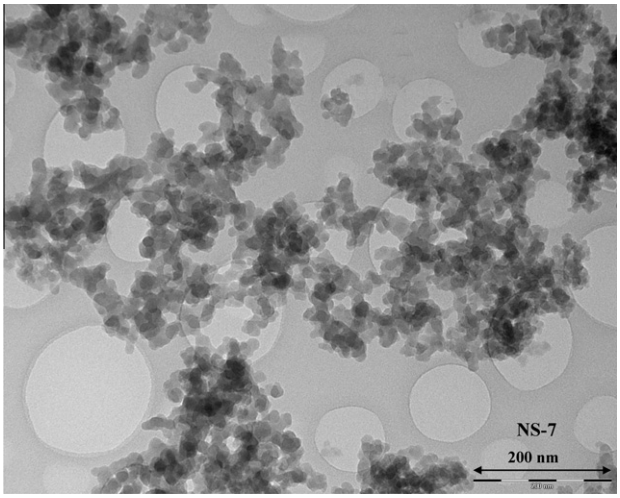

Fig. 8. TEM picture (89 kx) of the olivine nano-silica NS-7.

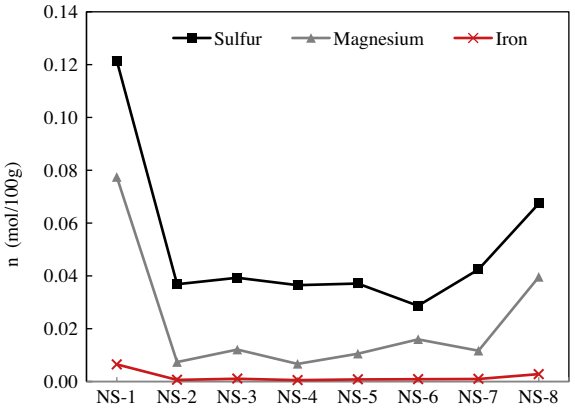

Fig. 9. Molar composition of sulfur, magnesium and iron of the olivine nano-silica (moles/100 g of sample).

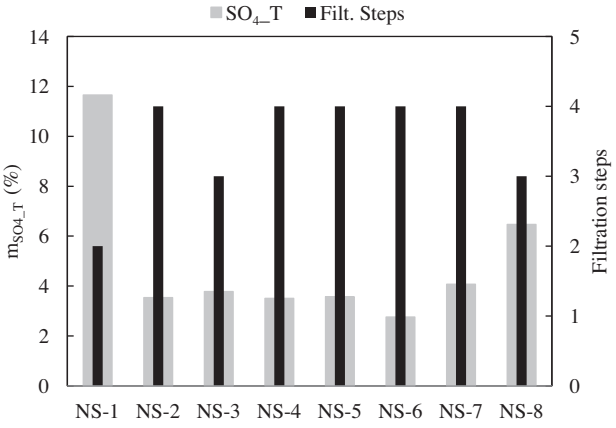

Fig. 10. Total sulfate and filtration steps of the olivine nano-silica.

respectively. The general trend is that the primary particle size decreases with the speed of reaction of olivine. Thus, when the dissolution of olivine is faster, the amount of silica released into the suspension is higher and the reaction time is shorter, resulting in silica particles of smaller diameter than when the reaction is slower.

In addition, the average pore diameter, d_{p_A} and d_{p_D}, is in the same range as the primary particles, showing that the porosity is due to the voids between the primary particles in the agglomerate. Therefore, olivine nano-silica can be considered as the agglomeration of primary particles and as a mesoporous material. In addition, the SSA_{MP} does not exhibit a particular trend regarding the SSA_{BET} (see Table 4) and the ratio SSA_{MP}/SSA_{BET} is almost constant, being in the interval 18–29.

The chemical composition of the olivine nano-silicas is shown in Table 5. The purity (P_{Si}) is calculated as the difference between 100 and all the impurities considering that sulfur is in the sulfate form. Thus, this value includes the content of silica and silanol, and it is above 95% except for NS-1 and NS-8.

Table 6 shows the number of moles of sulfur, n_S, magnesium, n_{Mg}, and iron, n_{Fe}, together with the mass of total sulfate, $m_{SO_4\_T}$, the mass of sulfate related with olivine, $m_{SO_4\_ol}$, the mass of free sulfate, $m_{SO_4\_H_2SO_4}$, and the ratio magnesium/metal ions. The term $m_{SO_4\_T}$, refers to the equivalent amount of sulfate salts ($MgSO_4$ and $FeSO_4$). The free or extra sulfate, $m_{SO_4\_H_2SO_4}$ is calculated from the difference between $m_{SO_4\_T}$ and $m_{SO_4\_ol}$. The n_S, n_{Mg} and n_{Fe} are plotted in Fig. 9. The $m_{SO_4\_T}$ and the filtration steps carried out for the different samples are shown in Fig. 10. The number of moles of these three components follows a similar trend, exhibiting higher sulfate values (and also magnesium and iron values) for samples with fewer washing steps.

The $m_{SO_4\_T}$ decreases with the filtration steps, as can be observed in Fig. 10. In addition, the free sulfate could be easily removed adding extra filtration steps with distilled water. Therefore, additional steps of washing with water would reduce the total sulfate, increasing the purity of the nano-silica. In fact, some additional experiments (which are not reported here) with six washing steps, the last three of them with distilled water, have shown purities above 99%.

Another interesting point is that the ratio of magnesium/metal ions in the silica remains stable with an average value of 0.93, this value being almost identical to the value reported for forsterite content for Norwegian olivine, 0.92 [34]. It means that the magnesium and iron salts are adsorbed on the nano-silica with the same ratio as present in the olivine and that they are desorbed with the same ratio during washing as well.

5.4. Process yield of the olivine nano-silica

The TG analyses of NS-1, NS-2, NS-5 and NS-8 and the DTG of NS-1are shown in Fig. 11. The higher mass loss of NS-1 is related

Table 6
Sulfate content and ratio magnesium/metal ions of the olivine nano-silica.

Sample	n_S (mol/100 g)	n_{Mg} (mol/100 g)	n_{Fe} (mol/100 g)	m_{SO4_T} (%)	m_{SO4_ol} (%)	$m_{SO_4\_H_2SO_4}$ (%)	$n_{Mg}/(n_{Fe}+n_{Mg})$
NS-1	0.121	0.077	0.006	11.655	8.05	3.60	0.92
NS-2	0.037	0.007	0.001	3.535	0.77	2.77	0.92
NS-3	0.039	0.012	0.001	3.775	1.26	2.51	0.92
NS-4	0.036	0.007	0.001	3.506	0.69	2.82	0.93
NS-5	0.037	0.011	0.001	3.565	1.09	2.48	0.93
NS-6	0.029	0.016	0.001	2.756	1.62	1.14	0.95
NS-7	0.042	0.012	0.001	4.075	1.21	2.86	0.92
NS-8	0.067	0.040	0.003	6.472	4.07	2.40	0.93

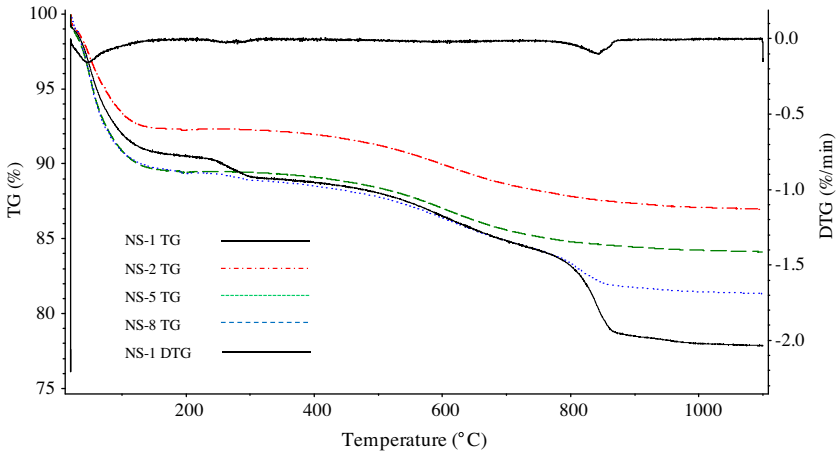

Fig. 11. TG and DTG analyses of the olivine nano-silica.

Table 7
The silica content and the purity of silica (P_{Si2}) of the olivine nano-silica.

Sample	m_{1100} (%)	m_{MgO} (%)	m_{FeO} (%)	m_{20-120} (%)	$m_{H_20\_A}$ (%)	m_{OH} (%)	m_{SiO_2} (%)	P_{Si2} (%)
NS-1	77.86	3.12	0.46	8.59	9.34	4.19	81.26	87.80
NS-2	86.96	0.30	0.05	7.27	7.76	4.36	93.41	98.74
NS-3	85.20	0.48	0.08	8.25	9.09	3.95	92.25	97.68
NS-4	87.17	0.27	0.04	6.78	7.24	4.43	93.18	98.53
NS-5	84.13	0.42	0.06	9.81	10.52	4.07	92.75	98.24
NS-6	85.84	0.64	0.06	9.38	9.65	2.87	93.94	97.65
NS-7	89.85	0.47	0.07	3.65	4.38	4.46	92.69	98.15
NS-8	81.34	1.60	0.20	9.81	10.66	3.80	88.20	94.01

$m_{H_20\_A}$ is the water loss between 20 and 200 °C and m_{OH} is the water loss in the range of 400–1000 minus m_{MgO} and m_{FeO}.

Table 8
Process yield and separation efficiency of the olivine nano-silica.

Sample	$m_{NS\_exp\_im}$ (g)	m_{NS_exp} (g)	m_{NS_th1} (g)	Y_{NS} (%)	m_{NS_th2} (g)	E_{Sep} (%)
NS-1	26.72	21.71	40.16	54.06	38.20	56.84
NS-2	39.61	37.00	45.71	80.95	43.61	84.84
NS-3	31.91	29.44	44.51	66.13	40.35	72.96
NS-4	35.00	32.61	41.19	79.18	39.30	83.00
NS-5	36.70	34.04	44.95	75.73	43.42	78.39
NS-6	35.10	32.97	41.35	79.74	40.65	81.11
NS-7	39.01	36.16	43.66	82.81	40.84	88.53
NS-8	35.11	30.97	44.44	69.69	43.45	71.27

to the higher amount of sulfates. The TG curves of NS-3, NS-4, NS-6 and NS-7 have a shape similar to the NS-5 curve, showing similar values of sulfates. Five TG analyses of the sample NS-3 were conducted showing an RSD of 5.0% in the loss of ignition between 400 and 1100 °C.

The process yield is obtained using Eq. (2), the separation efficiency is obtained using Eq. (7) and the purity (P_{Si2}), is calculated as the difference between 100 and all the impurities determined from the TG analysis. These parameters are shown in Tables 7 and 8. The values of purity obtained by the TG analyses are only slightly higher than the purity values calculated from the ICP analysis. This difference is because the sulfate content calculated from the ICP is slightly higher than these values from the TGA.

The nano-silica produced experimentally, theoretically and the process yield are plotted in Fig. 12. The yield was in the range of 66–83%, except for the first experiment where it was 54%. The separation efficiency, E_{sep}, was in the range 71–88 with the exception of the first experiment. The process yield is only slightly higher than the separation efficiency, which means that the main factor affecting the process yield is the separation efficiency, and that is because more than 90% of the olivine has reacted with the acid in every experiment (see Table 3). The separation efficiency for NS-1 was unexpectedly low, possibly due to the high value of [H^+]. Although in the present study nano-silica was produced with a higher yield than Jonckbloedt [6], this parameter should be even further improved, because around 30% of the produced material was lost during the filtration. In order to raise the nano-silica recovery, a more efficient separation process should be employed. The separation process depends on the properties of the silica cake obtained during the filtration and on the time involved in producing the filter cake, and the latter being controlled by the texture of the nano-silica. Thus, the faster a filter cake (of good filtration properties) is formed, the higher the yield will be.

The SSA_{BET} versus the E_{sep} is plotted in Fig. 13. The general trend is that the E_{sep} increases with the SSA_{BET}. Therefore, it can be stated that the specific surface area of nano-silica influences the separation efficiency. The yield of experiment NS-2 is depicted in a different color, because its values were higher than expected. The reason why the E_{sep} was higher than expected is the long aging time of this experiment compared with the short aging time of the rest of the

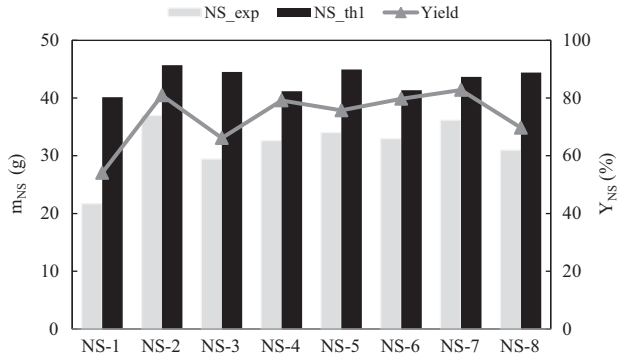

Fig. 12. Mass of the olivine nano-silica experimentally and theoretically as well as the process yield.

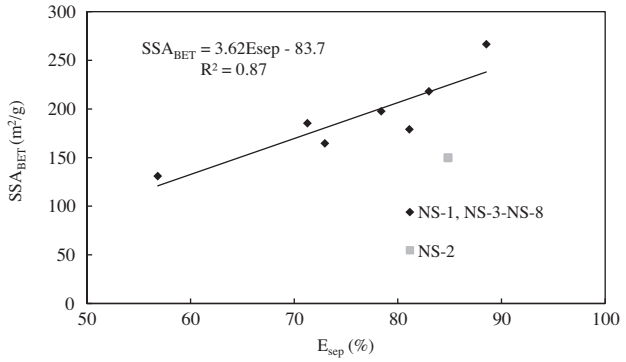

Fig. 13. Specific surface area of olivine nano-silica versus separation efficiency.

Table 9
Summary of the properties of different amorphous nano-silica [5,35].

Parameters	Pyrogenic	Precipitated	Lieftink	This work
Purity, SiO_2 (%)	>99.8	>95	–	>95
SSA_{BET} (m^2/g)	50–400	30–500	100-400	100–300
d (nm)	5–50	5–100	8–25	10–25
d_p (nm)	None	>30	>10	>10
Reference	Ecetoc	Ecetoc	Lieftink	–

experiments carried out at 50 °C. A plausible explanation for the phenomenon of increasing E_{sep} with the aging time would be that nano-silica particles agglomerate more with the aging time, forming the filter cake faster and losing less material. However, the primary particle size of the material does not change during the aging. In other words, the specific surface area of nano-silica remains constant, but larger clusters are formed facilitating the filtration and enhancing the silica yield. This phenomenon could be used to improve (time and efficiency) the separation efficiency of the nano-silica.

5.5. Comparison of different amorphous nano-silicas

Table 9 summarizes the physical and chemical properties of pyrogenic silica [35], precipitated silica [35], olivine silica produced by Lieftink [5] and the olivine nano-silica produced in the current study. All of them have a purity above 95%, a high SSA and a low particle size. Olivine nano-silica is the material with lower pore size diameter and higher mesoporosity. The main difference between the two olivine nano-silicas is that the nano-silica prepared here features a slightly smaller specific surface area than Lieftink's nano-silica. This difference in the surface area of olivine nano-silica is due to the kinetics of the dissolution of olivine and the content of impurities. Lieftink [5] produced nano-silica with faster kinetics, as we can see from the reaction times in Tables 1 and 3. Because the temperature and concentration of sulfuric acid are the same, the surface area of olivine is the factor that speeds up the kinetics. Additional filtration steps would increase the specific surface area and reduce the content of impurities.

An XRF analysis of the olivine nano-silica produced by Jonckbloedt [6] with waste sulfuric acid is shown in Table 10. The value of the loss of ignition includes the water condensed from the nano-silica as silanol groups. Considering that the mass of water released is around 5%, the silica content is still under 85%, which is much lower than the purity of our olivine nano-silica.

6. Conclusions

The synthesis of nano-silica by the dissolution of olivine is a feasible method to prepare amorphous mesoporous nano-silica. This nano-silica has a specific surface area between 100 and 300 m^2/g and a primary particle size between 10 and 25 nm. These particles are agglomerated in clusters forming a mesoporous material with an average pore diameter between 17 and 28 nm. The impurity content is below 5% and can be further decreased by adding extra washing steps using water.

The specific surface area of olivine nano-silica depends on the kinetics of the reaction of olivine and the amount of magnesium sulfate in the porous solution. Thus, increasing the temperature, the surface area of olivine, the activity of the hydrogen ion and/or the number of washing steps results in an increase in the nano-silica surface area. In this way, different types of nano-silica can be produced by changing the process conditions.

The separation efficiency increases with the specific surface area of nano-silica and aging time. Even if the E_{sep} is higher than the one reported by Jonckbloedt [6], it could still be improved by speeding up the formation of the cake during the filtration and/or modifying the properties of the cake. One way to do that is to keep the slurry aging for several hours before the filtration. Thus, the nano-silica agglomerates, leading to a more efficient separation process. Another possibility would be to add a recovery step to the process.

The results shown here demonstrate that the dissolution of olivine in sulfuric acid is a feasible method to produce an amorphous mesoporous nano-silica. In addition, the low energy requirement makes it possible to use this material in new fields where previously its price was prohibitive. Therefore, the olivine dissolution process is a convenient alternative to the traditional methods of nano-silica production.

Acknowledgments

The authors wish to express their appreciations to Dr. D.J. Lieftink, Dr. R.C.L. Jonckbloedt, Dr. A.J.J. van der Zanden and R.J. van Enk for their fruitful discussions and comments. They furthermore express their gratitude to EU FP7 project ProMine: Nano-particle

Table 10
Chemical analysis of the olivine nano-silica produced by Jonckbloedt [6].

SiO_2	Al_2O_3	Fe_2O_3	MnO	MgO	CaO	Na_2O	K_2O	TiO_2	P_2O_5	LOI
78.5	<0.22	0.19	<0.006	0.3	<0.13	0.21	<0.05	2.09	0.01	11.94

products from new mineral resources in Europe (Grant Agreement No. 228559) and to the Materials innovation institute - M2i (Project number M81.1.09338). The authors also wish to express their gratitude to following sponsors of the Building Materials group at TU Eindhoven: Bouwdienst Rijkswaterstaat, Graniet-Import Benelux, Kijlstra Betonmortel, Struyk Verwo, Attero, Enci, Provincie Overijssel, Rijkswaterstaat Directie Zeeland, A&G Maasvlakte, BTE, Alvon Bouwsystemen, V.d. Bosch Beton, Selor, Twee "R" Recycling, GMB, Schenk Concrete Consultancy, Intron, Geochem Research, Icopal, BN International, APP All Remove, Consensor, Eltomation, Knauf Gips, Hess ACC Systems and Kronos (chronological order of joining).

References

[1] O.W. Flörke, H.A. Graetsch, F. Brunk, L. Benda, S. Paschen, H.E. Bergna, W.O. Roberts, W.A. Welsh, C. Libanati, M. Ettlinger, D. Kerner, M. Maier, W. Meon, R. Schmoll, H. Gies, D. Shiffmann, Silica, Ullmann's Encyclopedia of Industrial, Chemistry, 2008.
[2] Freedonia. World Specialty Silicas, 2010.
[3] R.D. Schuiling. A method for neutralizing waste sulphuric acid by adding a silicate, US 1987/4707348, 1986.
[4] J. Van Herk, H.S. Pietersen, R.D. Schuiling, Neutralization of industrial waste acids with olivine – the dissolution of forsteritic olivine at 40–70°C, Chemical Geology 76 (1989) 341–352.
[5] D.J. Lieftink. The preparation and characterization of silica from acid treatment of olivine, PhD Thesis, Utrecht University, 1997.
[6] R.C.L. Jonckbloedt. The dissolution of olivine in acid, a cost effective process for the elimination of waste acids, PhD Thesis, Utrecht University, 1997.
[7] S. Olerud. Method for manufacturing spherical silica from olivine, US 1998/5780005, 1998.
[8] F. Hahn. Silica with High Silanol Group Content, NL19971007131 19970926; 1999.
[9] T. Hansen, B. Zander. Extraction of silica and magnesium compounds from olivine, WO Patent WO/2002/048,036; 2002.
[10] G. Gunnarsson, O. Wallevik, L. Ekornrod, B. Langseth, P. Engseth. Process for Production of Precipitated Silica from Olivine, US 2000/0263657; 2005.
[11] R.K. Iler, The Chemistry of Silica: Solubility, Polymerization, Colloid and Surface Properties, and Biochemistry, John Wiley and Sons, 1979.
[12] E.A. Gorrepati, P. Wongthahan, S. Raha, H.S. Fogler, Silica precipitation in acidic solutions: mechanism, pH effect, and salt effect, Langmuir 26 (2010) 10467–10474.
[13] B.A. Fleming, Kinetics of reaction between silicic acid and amorphous silica surfaces in NaCl solutions, Journal of Colloid and Interface Science 110 (1986) 40–64.
[14] L.W. Kelts, N.J. Effinger, S.M. Melpolder, Sol-gel chemistry studied by ^{1}H and ^{29}Si nuclear magnetic resonance, Journal of Non-Crystalline Solids 83 (1986) 353–374.
[15] M.K. Titulaer, M.J. den Exter, H. Talsma, J.B.H. Jansen, J.W. Geus, Control of the porous structure of silica gel by the preparation pH and drying, Journal of Non-Crystalline Solids 170 (1994) 113–127.
[16] D.J. Lieftink, J.W. Geus, The preparation of silica from the olivine process and its possible use as a catalyst support, Journal of Geochemical Exploration 62 (1998) 347–350.
[17] D.I. Siegel, H.O. Pfannkuch, Silicate mineral dissolution at pH 4 and near standard temperature and pressure, Geochimica et Cosmochimica Acta 48 (1984) 197–201.
[18] D.E. Grandstaff, S.M. Colman, D.P. Dethier (Eds.), The Dissolution Rate of Forsteritic Olivine from Hawaiian Beach Sand, Academic Press inc., 1986.
[19] R.A. Wogelius, J.V. Walther, Olivine dissolution kinetics at near-surface conditions, Chemical Geology 97 (1992) 101–112.
[20] A. Awad, A.F. Koster van Groos, S. Guggenheim, Forsteritic olivine: effect of crystallographic direction on dissolution kinetics, Geochimica et Cosmochimica Acta 64 (2000) 1765–1772.
[21] E.H. Oelkers, An experimental study of forsterite dissolution rates as a function of temperature and aqueous Mg and Si concentrations, Chemical Geology 175 (2001) 485–494.
[22] M. Hänchen, V. Prigiobbe, G. Storti, T.M. Seward, M. Mazzotti, Dissolution kinetics of fosteritic olivine at 90–150 °C including effects of the presence of CO_2, Geochimica et Cosmochimica Acta 70 (2006) 4403–4416.
[23] J.D. Hunt, A. Kavner, E.A. Schauble, D. Snyder, C.E. Manning, Polymerization of aqueous silica in H_2O–K_2O solutions at 25–200 °C and 1 bar to 20 kbar, Chemical Geology 283 (2011) 161–170.
[24] H.E. Bergna, W.O. Roberts, Colloidal Silica: Fundamentals and Applications, CRC, 2006.
[25] H. Tagawa, Thermal decomposition temperatures of metal sulfates, Thermochimica Acta 80 (1984) 23–33.
[26] M.J. Neil, P.E. Heckelman, C.B. Koch, K.J. Roman, The Merck Index, Merck Whitehouse Station, NJ, 2006.
[27] ISO 9277:2010, Determination of the Specific Surface Area of Solids by Gas Adsorption – BET Method, 2010.
[28] S. Brunauer, P.H. Emmett, E. Teller, Adsorption of gases in multimolecular layers, Journal of the American Chemical Society (1938).
[29] J.H. de Boer, B.G. Linsen, T. Osinga, Studies on pore systems in catalysts: VI. The universal *t* curve, Journal of Catalysis 4 (1965) 643–648.
[30] W.H. Harkins, G. Jura, Surfaces of solids. XIII. A vapor adsorption method for the determination of the area of a solid without the assumption of a molecular area, and the areas occupied by nitrogen and other molecules on the surface of a solid, Journal of the American Chemical Society (1944).
[31] E.P. Barrett, L.G. Joyner, P.P. Halenda, The determination of pore volume and area distributions in porous substances. I. Computations from nitrogen isotherms, Journal of the American Chemical Society (1951).
[32] K.S.W. Sing, D.H. Everett, R.A. Haul, L.Moscous, R.A. Pierotti, J. Rouquerol, T. Siemieniewska, Reporting physisorption data for gas/solid systems with special reference to the determination of surface area and porosity, Pure and Applied Chemistry (1985).
[33] S.J. Gregg, K.S.W. Sing. Adsorption, Surface Area and Porosity, 1991.
[34] R. Osland. Modelling of variation is Norwegian olivine deposits (Causes of variation and estimation of key quality factors), PhD Thesis, 1997.
[35] ECETOC. M. Gribble (Ed.), Synthetic Amorphous Silica (CAS No. 7631-86-9), Joint Assessment of Commodity Chemicals (JACC) Report No. 51, 2006.